Photochemical & Photobiological Sciences

PAPER

View Article Online
View Journal | View Issue

Cite this: *Photochem. Photobiol. Sci.*, 2014, **13**, 1052

"Turn-on" fluorescent chemosensor for zinc(II) dipodal ratiometric receptor: application in live cell imaging†

Kundan Tayade,[a,b] Banashree Bondhopadhyay,[c] Hemant Sharma,[d] Anupam Basu,[c] Vikas Gite,[a] Sanjay Attarde,[b] Narinder Singh*[d] and Anil Kuwar*[a]

Received 4th February 2014,
Accepted 24th March 2014

DOI: 10.1039/c4pp00034j

www.rsc.org/pps

A dipodal ligand 2,2′-((ethane-1,2-diylbis(azanediyl))bis(ethane-1,1-diyl))diphenol was synthesized through a condensation reaction and was characterized with IR, ^{1}H NMR, ^{13}C-NMR, and mass spectroscopy. The receptor **2** has shown marked enhancement in fluorescence intensity (emission signal at 341 nm) on binding with Zn^{2+} as compared to other surveyed metal ions. The sensor has shown dramatic changes in dual channel fluorescence emission with λ_{max} at 300 and 341 nm. The successive addition of Zn^{2+} to the solution of the sensor led to a blue shift of the peak maxima and interestingly upon addition of higher equivalents of Zn^{2+} quenched the fluorescence intensity of the sensor, and ultimately the original fluorescent profile of sensor was restored. The structures of **2** and **3** were optimized with B3LYP/LanL2DZ basis sets. The receptor **2** successfully detect the Zn^{2+} ion in HeLa cells cultured in Zn^{2+} enriched medium.

Introduction

The research arena of supramolecular chemistry is focusing towards the synthesis of simple, cost effective noncyclic receptors; which aids the fluorescence-based detection of physiologically important metal ions.[1–5] Several metal ions play a crucial role in physiological processes as long as they do not exceed the cellular needs.[6–9] Zn^{2+} has an indispensable role in many biological processes such as being involved in stimulation of more than 100 enzymes in the body.[10–13] Nowadays, the role of Zn^{2+} in neurobiology has been thoroughly explored; such as, neuronal passing can occur as a result of abandoned Zn^{2+} ion released after a stressful brain injury, stroke, or seizure.[14–16] Zn^{2+} also stimulates the production of α-amyloid leading to Alzheimer's disease and other neurological threats.[17] Moreover, the excess of Zn^{2+} present in the soil may lead to suspending the activities of several important microbes. Regulated amounts of Zn^{2+} are important for the physiological functioning of the flora and fauna;[18] thus Zn^{2+} is often considered as an interesting paradox to life and highlights the importance of detection methods for Zn^{2+} recognition in environmental and biological samples.

The deficiency of proper detecting probes for over a quite large concentration range and exhibiting high binding affinity is a severe inhibition to further surveys of this metal ion.[19] Most of the reported sensors for Zn^{2+} ion show deprived binding affinity towards Zn^{2+} ion and suffer strong interference effects.[20,21] Significant effort has been dedicated to the improvement of Zn^{2+} selective fluorescent receptors in the last decade. However, in most cases fluorescence changes can only be observed in non-aqueous solvents and are affected by the common interference of other cations, which bound the limits of their analytical application in environmental real samples. Therefore, the development of a highly sensitive and selective fluorescent receptor for Zn^{2+} ion in aqueous solution is very important and is still a stimulating task for the researchers.[22]

Herein, we explored the new application of receptor **2** as cation sensor with "Turn-ON" mechanism based upon the concentration of the metal ion. It merits mentioning that, as compared to the previously reported receptors for Zn^{2+} our synthesized receptor shows a comparable affinity towards the zinc ion with a low detection limit.[23–27]

Experimental

General information

IR spectra were recorded on a Perkin Elmer Spectrum one spectrometer, using Nujol Mull. ^{1}H and ^{13}C NMR spectra were

[a]*School of Chemical Sciences, North Maharashtra University, Jalgaon, 425001 MS, India. E-mail: kuwaras@gmail.com*
[b]*School of Environmental and Earth Sciences, North Maharashtra University, Jalgaon, 425001 MS, India*
[c]*Molecular Biology and Human Genetics Laboratory, Department of Zoology, The University of Burdwan, Burdwan, West Bengal, India*
[d]*Department of Chemistry, Indian Institute of Chemistry, Ropar, Rupnagar, Punjab, India. E-mail: nsingh@iitrpr.ac.in*
†Electronic supplementary information (ESI) available. See DOI: 10.1039/c4pp00034j

obtained on a Bruker AVANCE DMX400 spectrometer in DMSO-d_6 as solvent. Fluorescence measurements were made with a HORIBA JOBIN YVON, Fluoromax-4 Spectrofluorometer. UV-Vis absorption spectra were recorded on Shimadzu UV-2450 spectrophotometer. The fluorescence images were recorded on Leica DM 1000 fluorescence microscope using UV filter (Excitation–UV, Band Pass range: 340–380 nm, Dichromatic Mirror: 400 nm) and Green Filter (Excitation–Green, Band Pass range: 515–560 nm, Dichromatic Mirror: 580 nm). Thermal analysis study was carried out on Perkin Elmer DSC 400 and Perkin Elmer TGA 400. The solvents were distilled before use to ensure purity. Commercially available reagents were used without further purification.

Synthesis of receptor 2. Compound **1** was synthesized by refluxing one mole of ethane-1,2-diamine (0.60 g, 10 mmol) with two equivalents of 2-hydroxy acetophenone (2.72 g, 20 mmol) in ethanol (50 ml). Compound **1** was obtained with good yield and appears as yellow crystalline powder with 70% yield, mp > 250 °C. Further, receptor **2** was obtained from compound **1** by reduction of imine linkages with $NaBH_4$ in CH_3OH with good yield. Yield 81%, mp ≥ 250 °C. IR (KBr, cm^{-1}): ν = 3291, 2841, 2556, 1900, 1815, 1591, 1450, 1352, 1242, 1197, 1032, 968, 932, 873, 760 cm^{-1}; ^{1}H-NMR (300 MHz, $CDCl_3$): δ = 1.42–1.46 (d, 6H, 2-CH_3), 1.67–1.75 (bs, 2H, 2-OH), 2.72–2.80 (t, 4H, 2-CH_2–), 3.80–3.89 (q, 2H, 2═CH–), 6.74–7.17 (m, 8H, Ar–H), 11.38 (s, 2H, NH). ^{13}C NMR (75 MHz, $CDCl_3$ = few drops of DMSO): δ = 21.1, 46.8, 58.9, 116.5, 119.0, 126.4, 127.9, 128.2, 156.9. LC-MS (M + H^+) calcd for $C_{18}H_{25}N_2O_2$ = 301.19, found for $C_{18}H_{25}N_2O_2$ = 301.07. CHN Analysis; Calcd C, 71.97; H, 8.05; N, 9.33; Found C, 71.82; H, 8.19; N, 9.37.

Cation recognition studies

The cation recognition studies were performed at ambient temperature (25 °C), and the solution was repeatedly shaken before recording the absorption and emission spectra to ensure uniformity. The cation binding ability of receptor **2** was studied by adding fixed amounts (0.5 equivalent) of metal salts (1 mM) to a standard solution of receptor **2** (0.1 mM, 2 ml) in CH_3CN by keeping the solvent ratio constant throughout the experiment. The binding study was explored by using fluorescence spectroscopy.

UV-visible and fluorescence spectral measurements

For UV-Vis absorption and fluorescence spectroscopy, the metal ions Na^+, K^+, Mg^{2+}, Al^{3+}, Cs^+, Ba^{2+}, Ca^{2+}, Sr^{2+}, Fe^{3+}, Co^{2+}, Ni^{2+}, Cu^{2+}, Zn^{2+}, Cd^{2+}, Hg^{2+}, Pb^{2+}, Th^{4+}, Ag^+, and Bi^{3+} were added as their nitrates, Cr^{3+}, Mn^{2+} were added as their chlorides, while U^{6+} was added as its sulphate. The solutions of metal salts (1 mM) were prepared in CH_3CN containing 1% H_2O for analysis with receptor **2**. The solution of receptor **2** (0.1 mM) was freshly prepared in CH_3CN containing 1% H_2O. This solvent ratio was kept constant throughout the experiment. The excitation was carried out at 278 nm for receptor **2** with 5 nm emission slit widths in the fluorometer. For absorbance and fluorescence measurements 1 cm width and 3.5 cm height quartz cells were used.

In vitro cell imaging

Human cervical cancer cell HeLa was procured from the National Centre for Cell Science, Pune, India and cultured in DMEM medium supplemented with 10% FBS and 2% L-glutamine-penicillin-streptomycin and maintained at 37 °C in a humidified CO_2 incubator. The cells were seeded in the 35 mm culture dish with seeding density of 30×10^4 cells. After reaching 60% confluence, complete media was replaced with serum free media. Immediately the cells were treated with receptor **2** (2 μM) and incubated for 2 h. After washing the dish, fresh media was added and Zn^{2+} (25 μM) were also supplemented to the media. Live imaging of the cells was taken under florescence inverted microscope (Leica DMI 6000B) using UV and green excitation filter under 20× objective.

Results and discussion

2,2′-{Ethane-1,2-diylbis[nitrile(1*E*)eth-1-yl-1-ylidene]}diphenol (compound **1**) was synthesized by refluxing an ethanol solution of 2-hydroxyacetophenone and ethane-1,2-diamine (2 : 1 molar ratio) for 1 h. The reaction mixture was cooled and yellow coloured crystals of compound **1** were separated out. The crystals were filtered off and recrystallized from ethanol to give bright yellow crystals. Compound **1** was obtained with good yield.[21] Further, receptor **2** was synthesized through reduction of compound **1** with $NaBH_4$ (Scheme 1). The synthesized receptor **2** was characterized by the melting point, IR, ^{1}H-NMR, ^{13}C-NMR, mass spectroscopy (Fig. S1–4†).[28] The thermal behaviour of receptors **2** and **3** was studied using thermogravimetric analysis (TGA) and differential scanning calorimetry (DSC). TGA data show that the sharp endothermic peak for the decomposition of 2,2′-((ethane-1,2-diylbis(azanediyl))-bis(ethane-1,1-diyl))diphenol (**2**) and **3** was obtained at 246.89 and 122.68 °C respectively (Fig. S5a and b†).

The small initial weight loss in case of **3** may be attributed to the crystalline water molecule. DSC data depicted in Fig. S6a and b† revealed that the endothermic peak at 111.87 and 114.74 °C corresponds to the melting points of receptors **2**

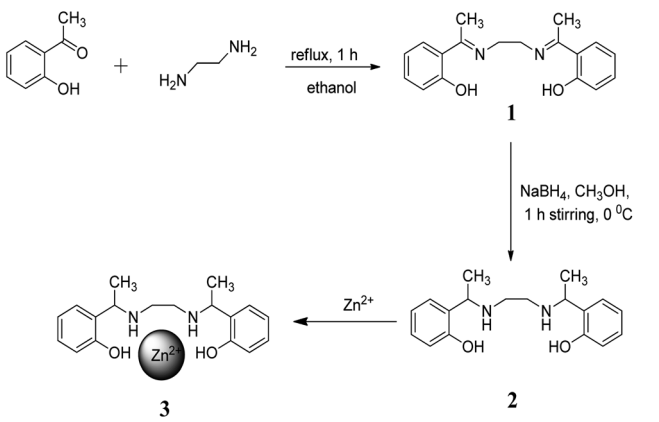

Scheme 1 Synthesis route of receptor **2** and **3**.

and **3**. The small peak obtained at 106.81 may be owing to the crystalline water molecule.

We tested the binding ability of receptor **2** by mixing it with Na^+, K^+, Mg^{2+}, Al^{3+}, Cs^+, Ba^{2+}, Ca^{2+}, Sr^{2+}, Cr^{3+}, Mn^{2+}, Fe^{3+}, Co^{2+}, Ni^{2+}, Cu^{2+}, Zn^{2+}, Cd^{2+}, Hg^{2+}, Pb^{2+}, Th^{4+}, Ag^+, Bi^{3+}, and U^{6+} metal ions in CH_3CN containing 1% H_2O. Receptor **2** exhibited fluorescence emission maxima at 300 and 341 nm upon excitation at 278 nm. The fluorescence was selectively and significantly enhanced in the presence of Zn^{2+} ion. There was no such distinct fluorescence peak observed in the emission outline of receptor **2** in the presence of other tested metal ions, which indicated the high selectivity of receptor **2** for Zn^{2+} ion (Fig. 1a). The enhancement of the fluorescence was attributed to strong complexation to form **3**, resulting in internal charge transfer (ICT) between the array of two phenolic moieties along with two amines and a zinc ion.[29,30] These four atoms constitute a tetrahedral pseudo cavity for selective binding with the zinc ion. The effect of increasing concentration of Zn^{2+} ion on the emission intensity of receptor **2** is pictured in Fig. S7a and b.† With increase of Zn^{2+} concentration, emission intensity increased drastically and reached saturation with 8-fold enhancement at 385 nm when 1 equiv. (200 μl) of Zn^{2+} was added. From the titration data, a dramatic change in the two emission maxima of receptor **2** at 300 and 341 nm was observed. Addition of Zn^{2+} up to 10 μl shows enhancement in both peaks with comparatively less enhancement assisting with blue shifting for the peak at 341 to 326 nm ($\Delta\lambda$ = 15 nm) (Fig. S7a†). With further addition of Zn^{2+} ion solution, the resurgence in fluorescence intensity of the emission peak shifted to 326 nm followed by restoring to its original position at 341 nm (upon addition of 100 μl Zn^{2+} ion solution), with a decrease in the emission peak at 300 nm assisted by a small red shift ($\Delta\lambda$ = 7 nm). Further proceeding of Zn^{2+} ion solution addition shows enhancement in the emission maximum at 341 nm and decrease in the emission intensity of the shifted peak at 307 nm. This provided a judicious pathway for chelation-enhanced fluorescence (CHEF) between the Zn^{2+} ion and receptor **2** (Fig. S7b†).[31] Also, the significant sensing of Zn^+ ion by receptor **2** may be attributed to the tetravalent pseudocavity within the synthesized key receptor.[32]

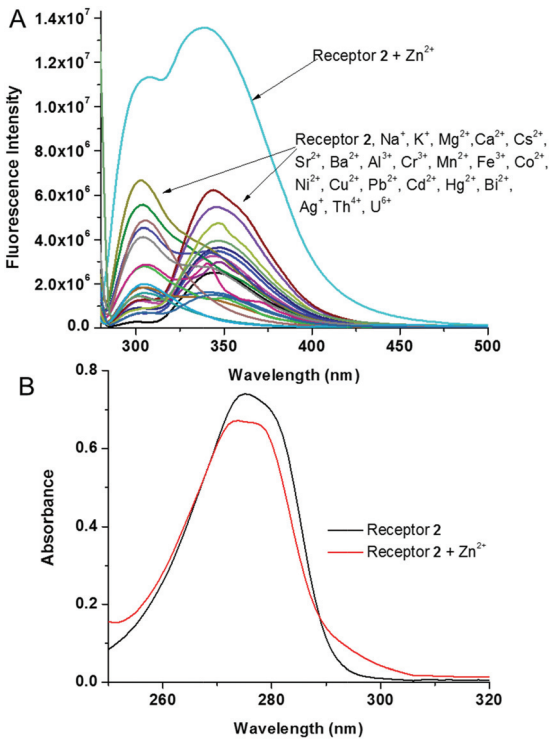

Fig. 1 (A) Fluorescence emission spectra of receptor **2** (0.1 mM) in the presence of different cations (1 mM), at excitation λ_{ex} = 278 nm. (B) Absorbance spectra of receptor **2** (0.1 mM) with and without Zn^{2+} ion in CH_3CN containing 1% H_2O.

The reason for these dramatic changes in the fluorescence intensity of two emission maxima shown by receptor **2** was explained by the mole plot pictured in Fig. S7c.† A fluorescence enhancement of up to 0.5 equivalent additions was revealed from the mole ratio plot and further small decrease indicates the formation of 2 : 1 complex between receptor **2** and Zn^{2+} and its subsequent dissociation. Further enhancement of up to 1 equivalent addition (200 μl) indicates 1 : 1 stoichiometry of **3**. Ongoing addition up to 2 equivalents indicates that fluorescence intensity is barely changed, showing the stability of the 1 : 1 complex formed (Fig. S7b and c†).

Also the spectrofluorometric response of receptor **2** towards various metal ions was recorded and depicted in Fig. S8† which shows that receptor **2** shows distinct fluorescence enhancement towards the Zn^{2+} ions as compared to other metal ions. To study the influence of other surveyed metal ions on Zn^{2+} ion binding with receptor **2**, we performed competitive experiments by mixing 2 equivalents of metal ions with 1 equivalent of Zn^{2+} ions (Fig. S9†). The observed fluorescence enhancement for mixtures of Zn^{2+} ion with surveyed metal ions was similar to that seen only for **3**. Thus no other metal ion appeared to interfere with the fluorescence intensity of **3**. These results indicate that receptor **2** shows significant sensitivity and selectivity towards Zn^{2+} ion over other studied competitive metal ions.

For practical reasons, the detection limit of receptor **2** for the analysis of Zn^{2+} ion was also an important parameter. Thus, based on the fluorescence titration measurement, the detection limit of receptor **2** for Zn^{2+} ion was found to be 0.65 μM.[33] The low detection limit might fully meet the requirements in biosensing and is comparable with literature reports as shown in Table S1.† The stoichiometry of **3** complexation was studied using Job's continuous variation method.[34] The plot between [HG] = $\{(\Delta F/F_0)[H]\}$ and $X_i = [H]_v/([H]_v + [G]_v)$ has maxima at X_i = 0.5 which represents the 1 : 1 stoichiometry for **3** complexation, which was also confirmed from the linear fitting of the normalized plot (Fig. S10a and b†). The stoichiometry of complexation was also confirmed by a Hill coefficient of 1.1446 obtained from a plot of $\log[(F - F_0)/(F_\infty - F)]$ *vs.* log[G] (Fig. S10c†).[35] In addition, the formation of 1 : 1 complex between **2** and Zn^{2+} was further confirmed by the appearance of a peak at 369.5, assignable to $[(\mathbf{2}\cdot Zn^{2+}-H^+)\text{-}(H_2O)_{0.5}]$ in the LC-MS (Fig. S11†). The formation of such a

Zn^{2+} complex can induce a π–π stacking interaction between the two phenyl rings leading to a rather rigid structure with quite strong fluorescence properties, as compared to the free receptor **2**.[36]

With the purpose of comprehending the metal-binding properties of receptor **2**, the binding constant (K_a) value was calculated by Benesi–Hildebrand,[37] Scatchard[38] and Connor's fitting[39] methodologies and the value found from the fluorescence data was $(1.00 \pm 0.1) \times 10^6\ M^{-1}$ which definitely made obvious the strong binding ability of **2** with Zn^{2+} (Fig. S12a–c†). The 1 : 1 binding ratio is also revealed from the linear fitting of the three methodologies. Further, to strengthen the coordination of Zn^{2+} ion complex, ^{1}H-NMR spectra of receptor **2** were recorded in the presence and absence of Zn^{2+} ion. It is observed that the signals of –OH proton at δ 1.67–1.75 get vanished upon addition of Zn^{2+} as shown in (Fig. S13†). These results clearly show that the –OH protons of receptor **2** forms coordination with Zn^{2+} ion. Further, the effect of pH has been studied on receptor **2** through varying the pH of the solution (Fig. S14†). It was observed that a change of pH did not produce any significant change in the fluorescence intensity of receptor **2** (Fig. S15†).

The fluorescence intensity of receptor **2** was recorded at different temperatures. With the increase of temperature, intensity was decreased and maximum intensity was observed at 25 °C as shown in Fig. S16.† Further, the response time was calculated to optimize the complexation time and has a response time of 41 s (Fig. S16†).

The absorption spectrum of receptor **2** upon addition of Zn^{2+} ion is shown in Fig. 1b. Receptor **2** exhibits peak maxima at 278 nm in CH_3CN. With the addition of Zn^{2+} ion into receptor **2**, there was no change in receptor **2**. This is a fact that the UV-Vis spectra of receptor **2** before and after the addition of 0.5 equivalent of Zn^{2+} showed a moderate change, illustrating that it bounds with the Zn^{2+} ion. Further, the titration was performed between Zn^{2+} and receptor **2** on UV-Visible spectrophotometer as shown in Fig. 2. We also tried to grow the single crystal of Zn^{2+} complex of receptor **2**. Unfortunately, we did not get crystals which are suitable for a diffraction study. Therefore, to comprehend the electronic environment and changes in the structure of receptor **2** upon complexation with Zn^{2+}, DFT calculation was performed using B3LYP/LANL2DZ basis set.[40–42] The optimized structure of receptor **2** has a more or less similar geometry (Fig. 3a). The two husks of receptor **2** having –OH groups are in opposite directions. The three electronegative atoms (O22, N26 and N25) arrange in a particular way for encapsulation of the analyte as shown in Fig. 3a. On complexation with Zn^{2+} ion, the two –OH groups which are in opposite directions come against each other (Fig. 3b). It is noticed that tetrahedral environment is constructed by oxygen and nitrogen atoms of –OH and –NH– groups for accommodation of Zn^{2+}. For more clarification and better understanding, a comparison of the geometrical parameters like bond length, bond angle and dihedral angle is made between **2** and **3** (Table S2†). On carefully examining this table, it is observed that there is a huge change in the geometry of receptor **2** on

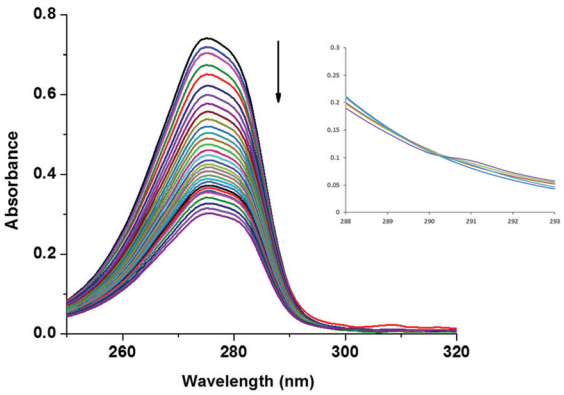

Fig. 2 Change in the absorbance spectra of receptor **2** upon continuous addition of Zn^{2+} ion in CH_3CN containing 1% H_2O; inset represent the isosbestic point of the titration.

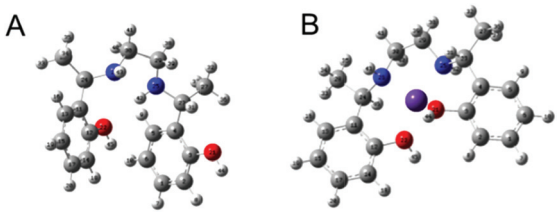

Fig. 3 The DFT optimized structure of: (a) receptor **2** and (b) **2**·Zn^{2+} calculated at the B3LYP/LANL2DZ level. The red, blue, gray, and purple spheres refer to O, N, C, Zn^{2+} atoms, respectively.

complexation with Zn^{2+}. A drastic change is observed in the dihedral angles of C5–C4–C23–N25, C3–C4–C23–N25 and O22–C12–C11–C24 as shown in Table S2.† It represents that atoms converge towards each other to form a pseudo cavity for Zn^{2+} ion. Further, all bond like N25–C29, C30–N26, C24–N26, C23–N25, C12–O22, C3–O21 showed an increase in the bond length upon addition of Zn^{2+} ion (Table S2†). Similarly, changes are observed in the bond angles (Table S2†).

To test these probabilities and to determine the amount of colocalizaton of the two fluorophores, we incubated HeLa cells with 2 μM receptor **2**. Subsequent imaging with a dual-filter fluorescence microscope afforded the images shown in Fig. 4. There was no fluorescence image observed when the cells were treated with receptor **2** alone, using a UV and green excitation filter. There was faint cellular fluorescence observed when the cells were imaged under UV excitation filter in the presence of the receptor **2** and Zn^{2+} (Fig. 4D).

On the contrary, a bright cellular image was observed when imaged under a green excitation filter in the presence of both receptor **2** and Zn^{2+} (Fig. 4E). Qualitative assessment of the images specifies a good intracellular overlap of the two fluorophores, an essential condition for the effectiveness of this sensing policy.

From the experimentation it is concluded that a simple new fluorescence receptor **2** was prepared successfully with a good yield. Receptor **2** has high sensitivity and selectivity for the Zn^{2+} ion. Receptor **2** shows a 8-fold fluorescence enhancement

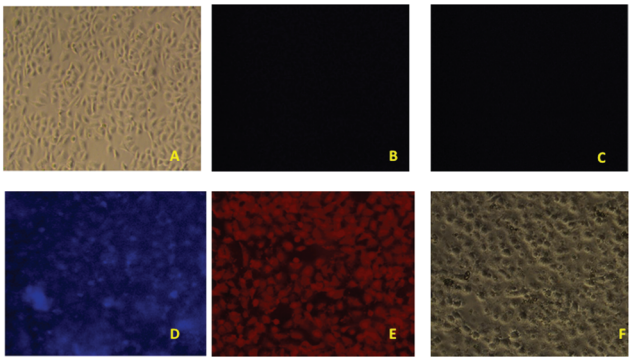

Fig. 4 Imaging of HeLa cells treated with receptor **2** and Zn^{2+}. (A) Phase contrast image of HeLa cells. (B) Fluorescence image of HeLa cells treated with receptor **2** (2 μM) (20×) and taken by UV excitation filter. (C) Fluorescence image of HeLa cells treated with receptor **2** (2 μM) (20×) and taken by green excitation filter. (D) Fluorescence photo-micrograph of HeLa cells incubated with receptor **2** (2 μM) and Zn^{2+} (25 μM) (20×) taken by UV excitation filter. (E) Fluorescence photo-micrograph of HeLa cells incubated with receptor **2** (2 μM) and Zn^{2+} (25 μM) (20×) taken by green excitation filter. (F) Phase contrast image of the cells treated with receptor **2** and Zn^{2+}.

in the presence of 1 equivalent Zn^{2+} ion, and is not significantly affected by the presence of common physiologically and environmentally important earth- and transition metal ions. The high binding affinity of the synthesized key receptor and its changing stoichiometry towards the sensing of Zn^{2+} ion with its increasing concentration are quite worth mentioning here. Confocal microscopy experiments show that receptor **2** can be used for noticing changes in Zn^{2+} levels within living HeLa cells. Future arrangements will hub on improving the optical brightness and binding sympathy of this third-generation sensor as well as applying receptor **2** and related chemical instruments to sensor the cell biology of zinc.

References

1 L. B. Desmonts, D. N. Reinhoudt and M. C. Calama, *Chem. Soc. Rev.*, 2007, **36**, 993.
2 R. Y. Tsien, in *Fluorescent and Photochemical Probes of Dynamic Biochemical Signals inside Living Cells*, ed. A. W. Czarnik, American Chemical Society, Washington, DC, 1993, 130.
3 A. P. de Silva, H. Q. Nimal Gunaratne, T. Gunnlaugsson, A. J. M. Huxley, C. P. McCoy, J. T. Rademacher and T. E. Rice, *Chem. Rev.*, 1997, **97**, 1515.
4 Z. Xu, J. Yoon and D. R. Chem, *Chem. Soc. Rev.*, 2010, **39**, 1996.
5 Q. Zhao, F. Li and C. Huanga, *Chem. Soc. Rev.*, 2010, **39**, 3007.
6 Y. D. Fernandez, A. P. Gramatges, V. Amendola, F. Foti, C. Mangano, P. Pallavicini and S. Patroni, *Chem. Commun.*, 2004, 1650.
7 F. Kratz and B. K. Keppler, *Metal complexes in cancer chemotherapy*, VCH, Weinheim, 1993.
8 V. Amendola, L. Fabbrizzi, F. Forti, M. Licchelli, C. Mangano, P. Pallavicini, A. Poggi, D. Sacchi and A. Taglieti, *Coord. Chem. Rev.*, 2006, **250**, 273.
9 R. R. Crichton, *Biological Inorganic Chemistry: An Introduction*, Elsevier, 2008.
10 E. Ochiai, *Bioinorganic Chemistry: A Survey*, Elsevier, 2008.
11 J. M. Berg and Y. Shi, *Science*, 1996, **271**, 1081.
12 J. H. Weiss, S. L. Sensi and J. Y. Koh, *Trends Pharmacol. Sci.*, 2000, **21**, 395.
13 R. M. Roat-Malone, *Bioinorganic Chemistry: A Short Course*, John Wiley & Sons, NJ, 2002.
14 S. W. Suh, J. W. Chen, M. Motamedi, B. Bell, K. Listiak, N. F. Pons, G. Danscher and C. J. Frederickson, *Brain Res.*, 2000, **852**, 268.
15 D. W. Choi and J. Y. Koh, *Annu. Rev. Neurosci.*, 1998, **21**, 347.
16 P. Roy, K. Dhara, M. Manassero, J. Ratha and P. Banerjee, *Inorg. Chem.*, 2007, **46**, 6405.
17 A. Takeda, *BioMetals*, 2001, **14**, 343; N. K. Wills, V. M. S. Ramanujam, N. Kalariya, J. R. Lewis and F. J. G. M. van Kuijk, *Eye Res.*, 2008, 878; L. C. Costello and R. B. Franklin, *Mol. Cancer*, 2006, **5**, 17.
18 J. Mertens, F. Degryse, D. Springael and E. Smolders, *Environ. Sci. Technol.*, 2007, **41**, 2992.
19 Y. Lv, M. Cao, J. Li and J. Wang, *Sensors*, 2013, **13**, 3131.
20 E. L. Que, D. W. Domaille and C. J. Chang, *Chem. Rev.*, 2008, **108**, 1517.
21 B. Valeur and I. Leray, *Coord. Chem. Rev.*, 2000, **205**, 3.
22 G. Q. Xie, Y. J. Shi, F. P. Hou, H. Y. Liu, L. Huang, P. X. Xi, F. J. Chen and Z. Z. Zeng, *Eur. J. Inorg. Chem.*, 2012, **162**, 327.
23 G. Sivaraman, T. Anand and D. Chellappa, *Analyst*, 2012, **137**, 5881–5884.
24 J.-A. Zhou, X.-L. Tang, J. Cheng, Z.-H. Ju, L.-Z. Yang, W.-S. Liu, C.-Y. Chena and D.-C. Baib, *Dalton Trans.*, 2012, **41**, 10626–10632.
25 P. Li, X. Zhou, R. Huang, L. Yang, X. Tang, W. Dou, Q. Zhao and W. Liu, *Dalton Trans.*, 2014, **43**, 706–713.
26 K. Kaur, M. Kaur, A. Kaur, J. Singh, N. Singh, S. K. Mittal and N. Kaur, *Inorg. Chem. Front.*, 2014, **1**, 99–108.
27 Z. Dong, X. Le, P. Zhou, C. Dong and J. Ma, *New J. Chem.*, 2014, **38**, 1802.
28 K. Tayade, J. Gallucci, H. Sharma, S. Attarde, R. Patil, N. Singh and A. Kuwar, *Dalton Trans.*, 2014, **43**, 3584.
29 Y. Maa, H. Chenb, F. Wanga, S. Kambama, Y. Wanga, C. Maoc and X. Chen, *Dyes Pigm.*, 2014, **102**, 301–307.
30 X. Peng, Y. Xu, S. Sun, Y. Wua and J. Fan, *Org. Biomol. Chem.*, 2007, **5**, 226–228.
31 F. Zapata, A. Caballero, A. Espinosa, A. Tárraga and P. Molina, *Dalton Trans.*, 2010, **39**, 5429–5431.
32 H. Sharma, N. Kaur and N. Singh, *Inorg. Chim. Acta*, 2012, **391**, 83–87.
33 X. Y. Liu, D. R. Bai and S. Wang, *Angew. Chem., Int. Ed.*, 2006, **118**, 5601.
34 P. Job, *Ann. Chim. Appl.*, 1928, **9**, 113.

35 L. Tang, M. Cai, P. Zhou, J. Zhao, K. Zhong, S. Hou and Y. Bian, *RSC Adv.*, 2013, **3**, 16802.
36 M. Shellaiah, Y.-H. Wu, A. Singh, M. V. R. Raju and H.-C. Lin, *J. Mater. Chem. A*, 2013, **1**, 1310–1318.
37 H. A. Benesi and J. H. Hildebrand, *J. Am. Chem. Soc.*, 1949, **71**, 2703.
38 G. Scatchard, *Ann. N. Y. Acad. Sci.*, 1949, **51**, 660.
39 K. A. Connors, *Binding constants, The measurements of molecular complex stability*, Wiley, New York, 1987.
40 C. Lee, W. Yang and R. G. Parr, *Phys. Rev. B: Condens. Matter*, 1988, **37**, 785.
41 P. J. Hay and W. R. Wadt, *J. Chem. Phys.*, 1985, **82**, 270.
42 F. Wang, R. Nandhakumar, J. H. Moon, K. M. Kim, J. Y. Lee and J. Yoon, *Inorg. Chem.*, 2011, **50**, 2240.